J|A|C|S ARTICLES

Published on Web 12/10/2009

Effect of Glass Dissolution on the Solution Deposition of ZnO Films and Its Exploitation for Deposition of Zn Silicates

Michael Kokotov,[†] Shay Bar-Nachum,[‡] Eran Edri,[†] and Gary Hodes*,[†]

Department of Materials and Interfaces, Weizmann Institute of Science, Rehovot 76100, Israel, and The Jerusalem College of Engineering, Jerusalem 91035, Israel

Received September 7, 2009; E-mail: gary.hodes@weizmann.ac.il

Abstract: ZnO is probably the most studied material deposited as films by aqueous solution methods. Both neutral and alkaline solutions are commonly used, and deposition is often carried out in glass vessels. We show that for depositions carried out under alkaline conditions, slow dissolution of the glass by the solution often results in formation of zinc silicates together with the ZnO. While this silicate formation is most clearly seen after long deposition times (many hours), it can be detected already within 1 h, while often ZnO depositions proceed for substantially longer. We also describe conditions where the zinc silicate deposits without formation of ZnO providing a method of depositing such films. Finally, we note that the glass of a reaction vessel also can affect deposition of CdSe, pointing to a more general role of this normally neglected parameter.

Introduction

ZnO is a readily available, nontoxic material that has many applications, both actual and potential. As such, it is the subject of very wide-ranging research. Of the numerous techniques used to prepare ZnO, solution methods have become very common, due to their simplicity and low temperatures. Chemical bath deposition (CBD)[1] is the most common solution process used to deposit films of ZnO. It has been developed considerably since it was first described for this purpose by Call et al. in 1980.[2] (Liquid phase deposition and hydrothermal deposition are terms also used for essentially the same process, the latter referring more generally to solids whether as films or as precipitates/powders.) While details of the mechanism may vary depending on deposition, the generally accepted mechanism is through dehydration of Zn−hydroxy complexes, which occur in the deposition solution, to form ZnO. The depositions are normally carried out at relatively high temperatures of 60−90 °C, which facilitate dissociation of the Zn complexes in the solution as well as dehydration. Despite its simplicity, CBD of ZnO has a tendency to suffer from problems of reproducibility, and it is often extremely sensitive to deposition conditions.[3] We previously showed how extremely low concentrations (<1 ppm) of "impurities" (Fe, Mn) in the CBD solution can form in situ nucleation centers on the substrate and allow film growth under conditions that would result in no deposit in the absence of the impurities.[4]

Most CBD processes are carried out in a glass vessel. Glass is known to be attacked by alkaline solutions. Despite this, the effect of this attack in a CBD process (which are often carried out at a fairly high pH) does not appear to have been considered to play an important role. In a continuation of our interest into causes of irreproducibilities in CBD, we show in this Article how the nature of the deposition vessel, specifically glass, can play a crucial role in the outcome of the ZnO deposition. The slowly dissolving SiO_2 network introduces silicate ions in the ZnO deposition solution, resulting in the formation of Zn silicates on the ZnO film.

While part of this Article is meant to demonstrate how one should be careful in the choice of the reaction vessel material, we also show how this knowledge can be exploited to deliberately deposit films of Zn silicates, either on top of ZnO or instead of ZnO. Zn-rich Zn silicate-containing coatings are widely used for corrosion protection of steel.[5] Because of its chemical stability and transparency in the ultraviolet and visible ranges, Zn silicate is also a commonly used material for phosphor preparation. Doped zinc silicate has high luminescence efficiencies, and it is widely used in cathode ray tubes and plasma display panels.[6] It is also used in laser crystals,[7] up-conversion luminescent materials,[8] and other electroluminescent devices.[9] Zn silicate for such devices is usually produced by solid-state reaction methods employing high temperature cofiring

[†] Weizmann Institute of Science.
[‡] The Jerusalem College of Engineering.

(1) Hodes, G. *Chemical Solution Deposition of Semiconductor Films*; Marcel Dekker: New York, Basel, 2003.
(2) Call, R. L.; Jaber, N. K.; Seshan, K.; Whyte Jr. *Sol. Energy Mater.* **1980**, *2*, 373.
(3) Govender, K.; Boyle, D. S.; Kenway, P. B.; O'Brien, P. *J. Mater. Chem.* **2004**, *14*, 2575.
(4) Kokotov, M.; Biller, A.; Hodes, G. *Chem. Mater.* **2008**, *20*, 4542.
(5) (a) Thomas, A. *Surf. Coat. Aust.* **2009**, *46*, 10. (b) Hemmings, E. *Surf. Coat. Aust.* **2005**, *42*, 12. (c) Vkhristyuk, P. N. *Fiz.-Khim. Mekh. Mater.* **1983**, *19*, 26.
(6) Blasse, G.; Grabai, B. C. *Luminescent Materials*; Springer-Verlag: Berlin, 1994.
(7) Veremeichik, T. F.; Zharikov, E. V.; Subbotin, K. A. *Cryst. Rep.* **2003**, *48*, 974. Translated from: *Kristallografiya* **2003**, *48*, 1042.
(8) Gerner, P.; Fuhrer, C.; Reinhard, C.; Gudel, H. U. *J. Alloys Compd.* **2004**, *380*, 39.
(9) (a) Horng, R. H.; Wuu, D. S.; Yu, J. W. *Mater. Chem. Phys.* **1997**, *51*, 11. (b) Ouyang, X.; Kitai, A. H.; Xiao, T. *J. Appl. Phys.* **1996**, *79*, 3229.

of ZnO and SiO_2 powders.[10] Alternative methods include RF magnetron sputtering,[11] spray pyrolysis,[12] sol−gel,[13] polymer precursor,[14] and various hydrothermal methods.[15] All of these publications (except refs 11 and 13b,c, which describe film deposition) describe the preparation of Zn silicate powders.

Experimental Section

Substrate Activation. In most experiments, the films were deposited on soda-lime glass microscope slides. (Other substrates, including various plastics and titanium, were also used with results similar to those of glass.) The substrates were rinsed with Millipore deionized water (DW) in an ultrasonic bath.

For the surface activation, the substrates were placed in glass vials filled with 0.5 mM fresh $KMnO_4$ solution.[16] 50 μL of *n*-butanol (as a reducing agent for the $KMnO_4$) per 20 mL of the permanganate solution was added. The vials were closed and placed in a water bath at 85 °C for 20−30 min. Permanganate-treated substrates were extensively rinsed in DW (the vials containing the samples were filled with DW, which was then poured out, and this was repeated for a total of 10 rinses) and then sonicated 5−10 min in DW in an ultrasonic bath. The extensive rinsing is important to prevent nucleation of ZnO in the bulk of the deposition solution from Mn-containing particles detached from the treated substrate. The activation allows facile nucleation due to adsorption of Zn species on the hydrated Mn oxide nuclei. In the absence of activation, little or no deposit forms.[16]

ZnO Film Deposition. Deposition solutions were prepared using the following aqueous stock solutions: 1.0 M $ZnSO_4$ (for some experiments, $ZnAc_2$, $ZnNO_3$, or $ZnCl_2$ was used), 4.0 M ammonium hydroxide, and 50% (by volume) monoethanolamine (2-aminoethanol). The final deposition solution was prepared from the stock solutions in 20 mL borosilicate glass vials (Wheaton liquid scintillation vials, part# 986541) or in polypropylene vials by sequential addition to water of 1.0 mL of zinc salt, ∼1.5 mL of ammonia, and 2 mL of ethanolamine, giving the following final concentrations: 0.1 M Zn^{2+} (unless otherwise stated), 1.7 M (10% v/v) ethanolamine, and ∼0.6 M NH_3 (some results are shown for films deposited using a lower ammonia concentration ∼0.5 M; this will be designated as "lower ammonia concentration"). The amount of water was chosen so that the total volume of each solution was 10 mL. The final pH was typically 11.0−11.2. For some experiments, crushed glass, either from the vials or from the soda-lime glass microscope slides, was added to some vials. Immediately after the solution preparation, the substrate was placed in the solution (slightly inclined from vertical to prevent particles, which might form in the solution from settling on the downward-facing side of the substrate, the side chosen for characterization). The reaction vial was closed and placed in a water bath at 75−95 °C. The deposition time varied from 0.5 to ∼350 h.

More details of the permanganate activation of the substrates and of the ZnO deposition have been described previously.[16]

Film Characterization. Films deposited on the bottom side of the substrates were first visually inspected to monitor coating uniformity on a macro scale. Scanning electron microscopy was carried out with a high resolution "Ultra 55" FEG Zeiss scanning electron microscope (SEM). Elemental analysis mapping was done by energy dispersive spectrometry (EDS) using an "OXFORD" detector in a SUPRA 55 VP FEG LEO SEM. Samples for cross-section transition electron microscopy (TEM) were prepared using an FEI Helios dual beam focused ion beam (FIB) system. TEM imaging and EDS analyses were done using a Philips CM120 TEM. X-ray diffraction (XRD) was carried out using a Rigaku RU300 rotating anode X-ray diffractometer.

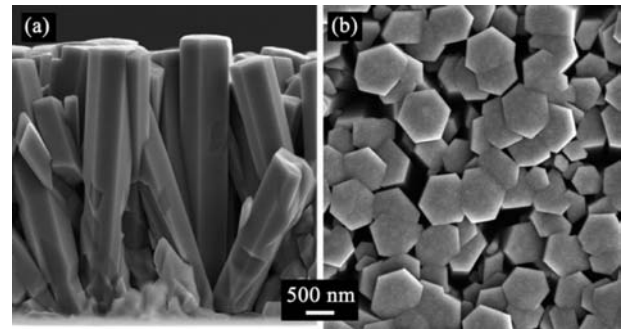

Figure 1. SEM cross-section (a) and plane view (b) of a ZnO film deposited at 92 °C for 40 min.

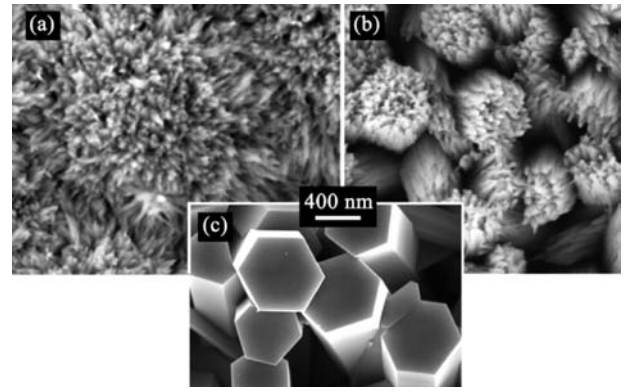

Figure 2. SEM images of ZnO films deposited at 90 °C for 1 h and kept in the deposition solution at 75−80 °C for 5 days: (a,b) in a glass vial ((a) dense ZnO film, (b) open morphology ZnO film from lower ammonia (complexant) concentration), (c) in a polypropylene vial.

Results

As shown in our previous work,[16] uniform ZnO films having typical morphology and crystal shapes shown in Figure 1 grow in about 40 min on substrates activated by permanganate. The areal density of the ZnO crystals and the film morphology (ZnO crystal size and aspect ratio and directionality/texture) can be tailored by varying activation conditions, the complexant:Zn concentration ratio, and by choice of the anion of the zinc salt. More recently, we found that increasing the pH of the deposition solution results in films with narrower ZnO crystals.

If, however, the deposition is continued for a much longer time, the morphology of the films changes significantly (Figure 2a,b). The films become very fibrous, and individual rods appear to be composed of many fibers. We initially thought that this

(10) (a) Schulman, J. H. *J. Appl. Phys.* **1946**, *17*, 902. (b) Brownlow, J. M.; Chang, I. F. *IEEE Trans. Electron Devices* **1983**, *ED-30*, 479. (c) Guo, Y.; Ohsato, H.; Kakimoto, K.-i. *J. Eur. Ceram. Soc.* **2006**, *26*, 1827.
(11) Minami, T.; Miyata, T.; Takata, S.; Fukuda, I. *Jpn. J. Appl. Phys.* **1991**, *30*, L117.
(12) Kang, Y. C.; Park, S. B. *Mater. Res. Bull.* **2000**, *35*, 1143.
(13) (a) Morimo, R.; Matae, K. *Mater. Res. Bull.* **1989**, *24*, 175. (b) Ji, Z.; Kun, L.; Yongliang, S.; Zhizhen, Y. *J. Cryst. Growth* **2003**, *255*, 353. (c) Copeland, T. S.; Lee, B. I.; Qi, J.; Elrod, A. K. *J. Lumin.* **2002**, *97*, 168. (d) Lin, J.; Sanger, D. U.; Mennig, M.; Barner, K. *Thin Solid Films* **2000**, *360*, 39.
(14) Su, K.; Tilley, T. D.; Sailor, M. J. *J. Am. Chem. Soc.* **1996**, *118*, 3459.
(15) (a) Ahmadi, T. S.; Haase, M.; Weller, H. *Mater. Res. Bull.* **2000**, *35*, 1869. (b) Lu, S. W.; Copeland, T.; Lee, B. I.; Tong, W.; Wagner, B. K.; Park, W.; Zhang, F. *J. Phys. Chem. Solids* **2001**, *62*, 777. (c) Yoon, C.; Shinboo, K. *J. Mater. Res.* **2001**, *16*, 1210. (d) Wang, H.; Ma, Y.; Yi, G.; Chen, D. *Mater. Chem. Phys.* **2003**, *82*, 414. (e) Wang, H.; Zhuang, J.; Peng, Q.; Li, Y. *J. Solid State Chem.* **2005**, *178*, 2332. (f) Xiong, L.; Shi, J.; Gu, J.; Shen, W.; Dong, X.; Chen, H.; Zhang, L.; Gao, J.; Ruan, M. *Small* **2005**, *1*, 1044. (g) Li, Q. H.; Komarneni, S.; Roy, R. *J. Mater. Sci.* **1995**, *30*, 2358. (h) Wan, J.; Chen, X.; Wang, Z.; Mu, L.; Qian, Y. *J. Cryst. Growth* **2005**, *280*, 239. (i) Zeng, J. H.; Fu, H. L.; Lou, T. J.; Yu, Y.; Sun, Y. H.; Li, D. Y. *Mater. Res. Bull.* **2009**, *44*, 1106.
(16) Kokotov, M.; Hodes, G. *J. Mater. Chem.* **2009**, *19*, 3847.

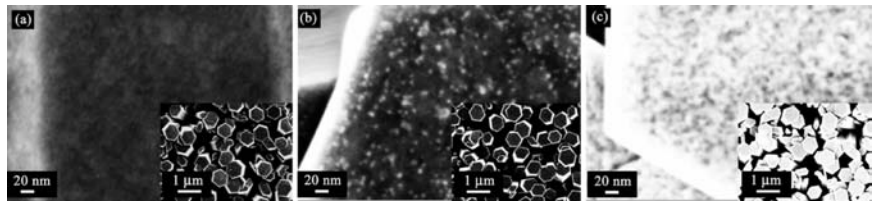

Figure 3. SEM images of ZnO films deposited at 90 °C (a) in a polypropylene vial − 3 h deposition; (b) in a glass vial − 1 h deposition; and (c) in a glass vial − 3 h deposition. The insets show lower magnification images. All three samples were placed together on one SEM sample holder, and all images were taken using identical SEM operating parameters, including contrast and brightness.

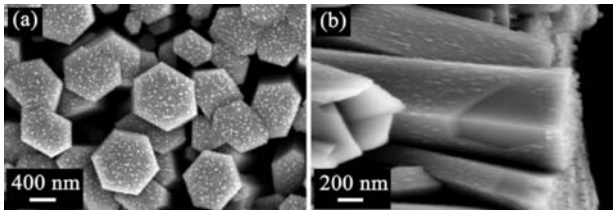

Figure 4. SEM images of a ZnO film deposited in a glass vial at 90 °C for 4 h and kept in the deposition solution at 80 °C for 4 h. (a) Plan view and (b) cross-section view.

fibrous structure was due to etching of the ZnO by the alkaline solution after the Zn^{2+} concentration in the deposition bath became low enough. However, under identical deposition conditions, when plastic vials were used in place of glass ones, this fibrous morphology did not occur (Figure 2c).[17]

A change in surface appearance of the initially deposited smooth ZnO rods is already seen by SEM imaging after 1 h of deposition. Figure 3b shows the formation of white "spots" some nanometers in size on the top of a ZnO rod grown for 1 h in a glass vial, suggesting formation of a different phase. The difference in contrast between the white spots and the darker ZnO is due to electric potential difference between the spots (different charging of the spots as compared to that of the ZnO; the in-lens secondary electron detector used is particularly sensitive to charging effects). The growth of these "spots" continues until, after 3 h of growth, a continuous layer of this phase is formed on the ZnO (Figure 3c). For films grown under identical conditions but in a plastic vial, no sign of this growth occurs (Figure 3a). After 4 h, growth of a separate layer on the sides of the ZnO rods, as well as on their tops, can be clearly seen (Figure 4). The nature of the growth of this fibrous layer depends on the morphology of the ZnO rods. Under conditions where open (loosely packed) ZnO rods form (in this case, by using a lower ammonia concentration), the layer grows on individual ZnO crystals (Figures 5a−c and 2b). For closer-packed ZnO rods, this overlayer coalesces to form a dense coating on the ZnO film (Figures 5d−f and 2a). This fibrous growth resembles the morphology of particles of Zn silicate powders obtained by hydrothermal methods (but at higher temperature than our deposition conditions) as described in refs 15d,h,f,i. The maximum thickness of the overlayer is achieved after about 3 days, depending on the solution temperature. A more spherical morphology of this overgrowth is obtained at slightly lower pH (10.8 instead of 11.0−11.2), as shown in Figure 6a. On occasion, such a morphology, or a morphology intermediate between that in Figure 6a and the more typical fibrous ones, is found even under standard pH conditions (Figure 6b,c). Such dual morphology behavior of Zn silicate is described in the hydrothermal literature, showing a greater tendency for spherical morphology at lower pH or at lower ammonia concentration,[15a,g,i] the same as we find for our films. This dual morphology behavior of zinc silicate was also found in synthesis from organic solutions.[18]

SEM backscattered images of such films clearly show that the overlayer on the ZnO has a lower average atomic number than that of the ZnO itself but higher that that of the glass substrate (Figure 7b together with the secondary electron image in Figure 7a). A cross-section EDS line scan through the film thickness (Figure 7c) shows that the overlayer consists of Si, Zn, and O in contrast to only Zn and O in the underlying film. It also shows that there is relatively more O and less Zn in the overlayer than in the ZnO underlayer. Cross-section TEM imaging of the film (Figure 7d−h) reveals a nanogranular structure (no crystal plane fringes were observed in the nanograins) of the overlayer (Figure 7f) and the single crystal nature of the ZnO rods (Figure 7g, which shows a smooth, featureless region of a ZnO crystal, and Figure 7h, a higher magnification image showing lattice fringes). The selected area electron diffraction patterns of the overlayer are very weak and broad but seem to match the powder pattern of ZnO. This indicates inclusions of some amount of ZnO nanocrystals in the apparently amorphous silicate phase. EDS/REM analysis of the overlayer gave an atomic % composition of: O ∼56%; Si ∼12%; Zn ∼32%. In most cases, XRD of these films does not reveal any additional phase besides the ZnO. However, in some samples, additional weak broad peaks and widening of the ZnO (100) peak were observed (Figure 8). The broad peaks can be best matched to a $Na_2Zn(Si_2O_6)$ phase.[19] No correlation was found between deposition condition or film morphology and appearance of these peaks. Annealing of the films at temperatures up to 500 °C (limited by the glass substrate) did not affect the XRD pattern. Combining all of the above results, together with the general observation from the literature that the most usual phase for hydrothermally grown zinc silicate is the willemite Zn_2SiO_4 phase, we consider that the most likely composition for this overlayer is the willemite phase with some inclusions of nanocrystalline ZnO and maybe also some sodium−zinc silicate phase. (Na usually is not reliably detected by EDS due to its tendency to evaporate under the electron

(17) We note that most of the results shown in this Article were obtained using $ZnSO_4$, but control experiments employing other zinc salts showed similar behavior, although with different rod diameters obtained depending on the anion of the Zn salt.[16]

(18) Lou, T. J.; Zeng, J. H.; Lou, X. D.; Fu, H. L.; Wang, Y. F.; Ma, R. L.; Tong, L. J.; Chen, Y. L. *J. Colloid Interface Sci.* **2007**, *314*, 510.

(19) There are at least dozens of alkali metal zinc silicate phases, each with a large number of peaks in the XRD pattern. Also, most well-defined XRD patterns in the literature of zinc silicate compounds in general are obtained after high-temperature annealing. A positive identification of the measured XRD patterns in our case is therefore less than reliable. The exact composition and phase is not of great relevance for this Article.

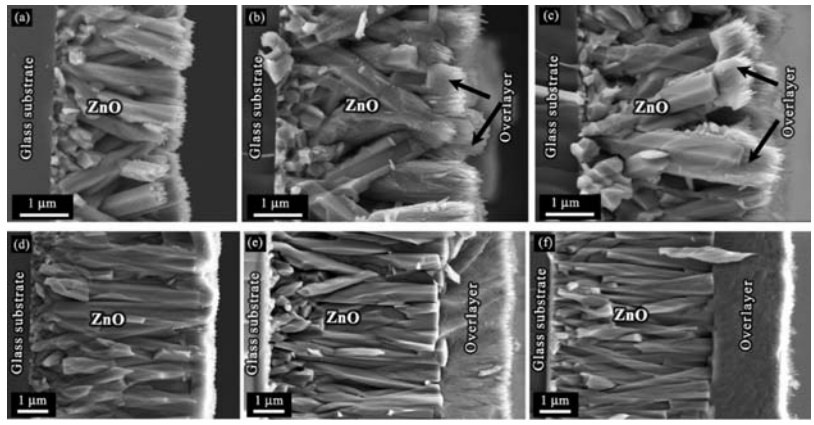

Figure 5. SEM cross-section views of two series of ZnO film depositions. (a−c) Films deposited from bath containing lower concentration of NH_3, less closely packed and less aligned ZnO rods after 24, 140, and 270 h deposition respectively; (d−f) normal concentration of NH_3, more closely packed and more vertically aligned ZnO rods after 13, 63, and 120 h deposition, respectively. Note the magnification is not identical for the two series.

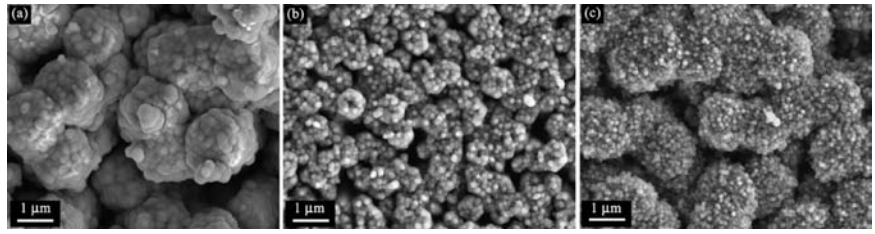

Figure 6. SEM images of depositions showing (a) a repeatable spherical morphology at lower pH − acid added. Occasional spherical morphology obtained using (b) low ammonia concentration and (c) normal ammonia concentration.

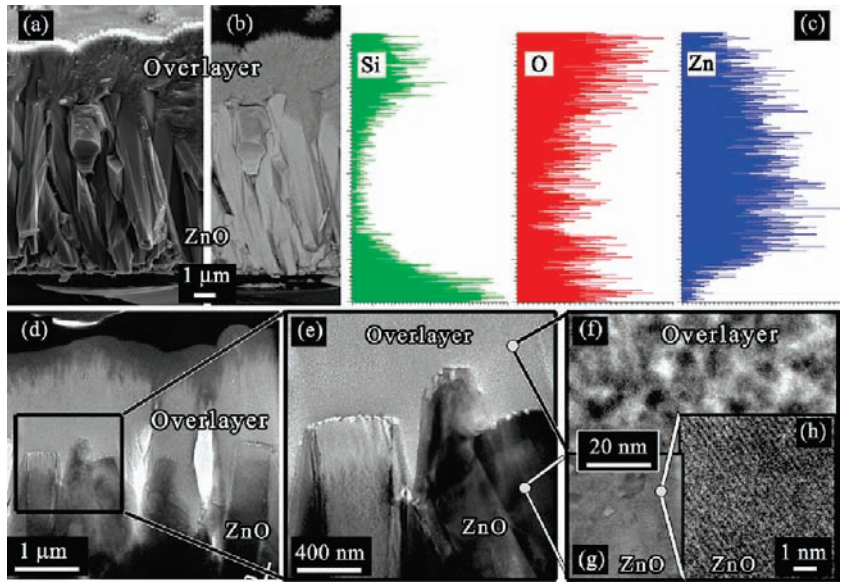

Figure 7. (a) Secondary electrons and (b) backscattered electron cross-section SEM images of dense ZnO film with thick overlayer. (c) SEM EDS line scan map across the film cross-section. (d−h) Cross-section TEM images of a similar film. (d) Upper parts of the ZnO rods covered with an overlayer (the dark gray and the black layers on top of the bright gray overlayer are metal films deposited for FIB lamella cutting). (e) Zoom-in of a section of (d). (f) Zoom-in of the overlayer. (g) Zoom-in of the ZnO crystal. (h) High magnification lattice image of the ZnO crystal.

beam.) If willemite and ZnO are indeed the two main phases, the semiquantitative TEM EDS results above are consistent with an average overlayer atomic composition corresponding to a calculated volume ratio of 85% amorphous Zn_2SiO_4 and 15% nanocrystalline ZnO.

As control experiments, pieces of broken glass (either from soda-lime glass microscope slides or borosilicate glass vials) were added to the deposition solution in plastic vials. The film morphology in these cases was similar to that obtained using glass vials. This provides additional proof that formation of the Si-containing overlayer is due to dissolution of glass. A larger amount of crushed glass or finer glass pieces added to a deposition solution result in faster formation of the crust overlayer, as expected. However, if sodium silicate is added to

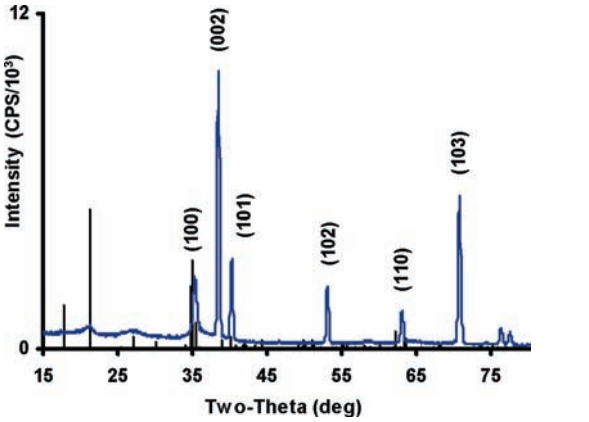

Figure 8. XRD pattern of ZnO film covered by an overlayer as in Figure 5e. All sharp peaks belong to ZnO. The vertical lines show the database pattern of the $Na_2Zn(Si_2O_6)$ phase (PDF#01-072-0741).

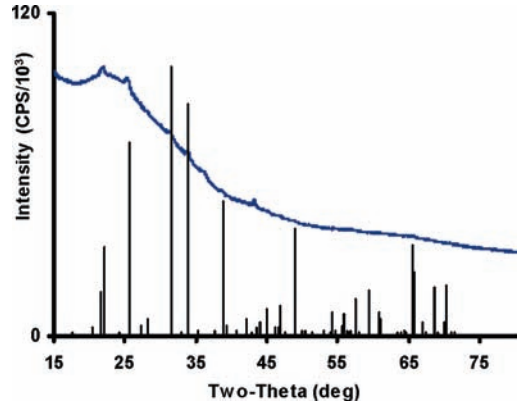

Figure 10. XRD pattern of an annealed (500 °C) film deposited using a low concentration (25 mM) of zinc, other conditions as standard. The vertical lines show the database pattern of the Zn_2SiO_4 (willemite, zinc silicate) phase (PDF#00-037-1485).

the deposition solution at the start of deposition, a precipitate forms immediately in the solution, and very little film formation occurs. Thus, slow release of silicate into the solution is necessary for film formation.

It might be asked why the glass substrate itself does not supply silicate ions to the deposition solution. ZnO deposition by CBD normally requires activation of the substrate to allow ZnO nucleation. While the glass substrates are activated (by permanganate treatment in this work), the vessel is not. Thus, the ZnO layer, which forms only on the activated substrate, protects it against dissolution.

We note that, for a long period of time, we were not aware of the silicate formation and thought that it was ZnO possessing a novel morphology. It was only after carrying out cross-section backscattered SEM (of particularly long depositions) that we realized there was a difference in composition between the ZnO and what we eventually realized was silicate and that some silicate already started to form even after short depositions, although this was not readily visible in its early stages in SEM imaging. Also, as noted above, the silicate would not be seen by XRD because no (or virtually no) XRD pattern is seen, even after thick layers of silicate had formed.

Using our deposition conditions, ZnO film growth is a fast process; it takes about 40 min until the ZnO film reaches its maximal thickness (this is faster than most other ZnO baths). We can reasonably assume that the silicate overlayer forms when the Zn^{2+} concentration drops below the concentration at which ZnO can continue to grow and an equilibrium is established between dissolution and growth of ZnO. If this assumption is true, then by starting with a low enough Zn^{2+} concentration (or high enough complex:Zn ratio), we should be able to obtain a predominantly or even solely Zn silicate film. Figure 9 shows SEM images of such films using 25% of the original Zn concentration (25 mM instead of 100 mM), all other components of the solution kept unchanged. Thin, apparently amorphous or very small crystal films were observed on the glass substrates using $ZnCl_2$ (or $ZnSO_4$) (Figure 9a,b). Extremely strong adhesion of the film to the substrate is indicated by the continuous crack lines, from the sample fracture, across the interface (Figure 9b). No XRD pattern was found from these as-deposited films. After being annealed at 500 °C for 1 h in air, two types of crystals could be seen in the SEM images: large ill-defined crystals inside the film (Figure 9d,f) and smaller faceted crystals embedded into the film surface (Figure 9e) (no atomic weight contrast is seen by backscattered imaging in either annealed or as-deposited films (Figure 9c,f)). Longer annealing at the same temperature did not change this picture. Weak XRD peaks indicating the presence of Zn_2SiO_4 (willemite zinc silicate) appeared after annealing (Figure 10).[19]

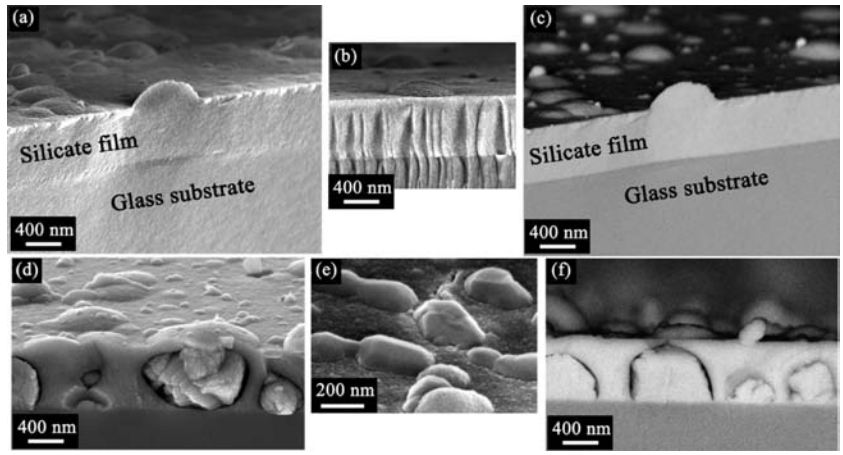

Figure 9. SEM secondary electron (a,b,d,e) and backscattered (c,f) images of a silicate film deposited using a low concentration of zinc (25 mM $ZnCl_2$). As deposited (a,b,c), annealed (d,e,f). Part (e) shows a zoomed-in region of the surface.

Finally, in view of our interest in nanoporous solar cells, we fabricated ZnO/CdSe/CuSCN solar cells using CBD ZnO on SnO_2-conducting glass.[20] Three cells were made using ZnO deposited in glass vials and three cells using ZnO deposited under identical conditions but in plastic vials. In all cases, the cells made in plastic vials gave open circuit voltages that were significantly higher (by $\geq$70 mV) than the control cells made using ZnO deposited in glass vials (the other cell parameters did not vary in any systematic way between the two types of ZnO). While preliminary, these experiments emphasize the importance of the nature of the reaction vessel in ZnO deposition.

Conclusions

Chemical bath deposition (CBD) of ZnO from alkaline solution in a glass reaction vessel gives initially ZnO, but an alkali metal Zn silicate phase forms as an overlayer on the ZnO as the Zn concentration in the bath decreases with time and this overlayer becomes thicker with increasing growth time. This phase forms due to slow etching of the glass vessel (both borosilicate and soda-lime glass behave similarly) at the pH of the solution (ca. 11). This etching gradually releases silicate ions to the solution, which react to give the silicate. Using plastic reaction vessels, only ZnO is formed regardless of the deposition time. While etching of glass in strongly alkaline solution is well-known, these results show that even under relatively mild alkaline condition, glass etching occurs and, more importantly, can completely change the nature of the deposit. Recently, we have noted that the influence of glass is not limited to ZnO depositions but that it is more general. Ion-by-ion deposition of CdSe, carried out under alkaline conditions from solutions containing nitrilotriacetic acid as a complexing agent,[21] proceeds much faster in a borosilicate vial than in a plastic one. Furthermore, if some pieces of soda-lime glass are introduced into such a bath, a substantial amount of Si is incorporated into the resulting films. The possibility of formation of silicates has to be taken into account because they can dramatically alter chemical, structural, and electronic properties of the deposited films. In preliminary experiments, the open circuit voltage of CdSe-sensitized ZnO nanoporous solar cells is increased considerably if the CBD ZnO is grown in a plastic vial as compared to a glass one.

We also present preliminary results that exploit this phenomenon to deliberately grow Zn silicate films, an important compound for luminescence and anticorrosion applications. In this case, a low starting concentration of Zn in the deposition solution prevents growth of ZnO, and only the silicate is formed as a very adherent film on glass substrates. Silicates of Zn cannot be grown simply by adding alkali metal silicate solution to the deposition bath as immediate precipitation occurs; the slow release of the soluble silicate is essential for this deposition. The source of the Si can be either the glass vessel itself or deliberately-added glass.

Acknowledgment. This work was supported by the US−Israel Binational Science Foundation and the Alternative Energy Research Initiative (AERI). We thank Dr. Yishay Feldman for help with XRD analysis, Dr. Palle von Huth for help with FIB sample cross-sectioning, and Dr. Ronit Popovitz-Biro for help with TEM imaging. The electron microscopy studies were conducted at the Irving and Cherna Moskowitz Center for Nano and Bio-Nano Imaging at the Weizmann Institute of Science. We acknowledge the Harold Perlman family's historic generosity.

JA907580U

(20) Levy-Clement, C.; Tena-Zaera, R.; Ryan, M. A.; Katty, A.; Hodes, G. *Adv. Mater.* **2005**, *17*, 1512.
(21) Gorer, S.; Hodes, G. *J. Phys. Chem.* **1994**, *98*, 5338.